Journal of Alloys and Compounds 501 (2010) 93–99

Contents lists available at ScienceDirect

Journal of Alloys and Compounds

journal homepage: www.elsevier.com/locate/jallcom

Crystallization behavior of $(1-x)Li_2O{\cdot}xNa_2O{\cdot}Al_2O_3{\cdot}4SiO_2$ glasses

Moo-Chin Wang[a], Chih-Wei Cheng[b], Kuo-Ming Chang[b], Chi-Shiung Hsi[c,*]

[a] Department of Fragrance and Cosmetic Science, Kaohsiung Medical University, 100 Shih-Chuan 1st Road, Kaohsiung 807, Taiwan
[b] Department of Mechanical Engineering, National Kaohsiung University of Applied Sciences, 415 Chien-Kung Road, Kaohsiung 80782, Taiwan
[c] Department of Materials Science and Engineering, National United University, 1 Lien-Da, Kung-Ching Li, Miao-Li 36003, Taiwan

ARTICLE INFO

Article history:
Received 21 January 2010
Received in revised form 5 April 2010
Accepted 7 April 2010
Available online 14 April 2010

Keywords:
Crystallization
Activation energy
Isothermal kinetics
Quantitative X-ray diffraction
$(1-x)Li_2O{\cdot}xNa_2O{\cdot}Al_2O_3{\cdot}4SiO_2$ glasses
Crystallization mechanism

ABSTRACT

The crystallization behavior of the $(1-x)Li_2O{\cdot}xNa_2O{\cdot}Al_2O_3{\cdot}4SiO_2$ glasses has been investigated using X-ray diffraction (XRD), scanning electron microscopy (SEM), transmission electron microscopy (TEM), electron diffraction (ED) and energy dispersive spectroscopy (EDS). The crystalline phase was composed of β-spodumene. The isothermal crystallization kinetics of β-spodumene from the $(1-x)Li_2O{\cdot}xNa_2O{\cdot}Al_2O_3{\cdot}4SiO_2$ glasses has also been studied by a quantitative X-ray diffraction method. The activation energy of β-spodumene formation decreases from 359.2 to 317.8 kJ/mol when the Na_2O content increases from 0 to 0.4 mol and it increases from 317.8 to 376.9 kJ/mol when the Na_2O content increases from 0.4 to 0.6 mol. The surface nucleation and plate-like growth were dominant in the crystallization of the $(1-x)Li_2O{\cdot}xNa_2O{\cdot}Al_2O_3{\cdot}4SiO_2$ glasses.

1. Introduction

Lithium–aluminum–silicate glass–ceramics have been extensively investigated and commercialized because of very low thermal expansion and excellent thermal and chemical durability. They are used practically as cooktop panels, stove windows, cookware and some precision parts [1]. The peculiar properties of these glass–ceramics are due to the framework structure of aluminosilicate tetrahedra which are the main crystalline phases. This crystal structure has very low bulk thermal expansion and also possesses low thermal expansion with consequent benefit of exceptional thermal stability and thermal shock resistance [2]. Glass–ceramics consisting of fine crystals of β-spodumene ($Li_2O{\cdot}Al_2O_3{\cdot}4SiO_2$, LAS_4) and β-eucryptite ($Li_2O{\cdot}Al_2O_3{\cdot}2SiO_2$, LAS_2) are of particular importance from a technological standpoint in that it encompasses such properties [3]. As that β-eucryptite is structurally similar to β-quartz which is a high temperature or to quartz and unstable at ambient temperature. β-spodumene is derived from keatite which is a form of silica that can only be prepared under hydrothermal condition [4,5].

The phase relation and properties of the $Li_2O{\cdot}Al_2O_3{\cdot}SiO_2$ system have received a great deal of attention during the past five decades [4–10]. Furthermore, the crystallization and properties of $Li_2O{\cdot}MgO{\cdot}Al_2O_3{\cdot}SiO_2$ [11,12] and $Li_2O{\cdot}CaO{\cdot}Al_2O_3{\cdot}SiO_2$ [13–18] glass–ceramics have been discussed in detail. The effect of Na_2O substation on the structure and properties of $(1-x)Li_2O{\cdot}xNa_2O{\cdot}Al_2O_3{\cdot}4SiO_2$ glasses has also been reported by Wang et al. [16]. However, an extensive literature search shows that the detail of the crystallization behavior of $(1-x)Li_2O{\cdot}xNa_2O{\cdot}Al_2O_3{\cdot}4SiO_2$ glasses has not been elaborated so far.

On the other hand, the dissolution and crystallization kinetics of a β-spodumene glass–ceramic has been reported by Dalal and Raj [17]. They have demonstrated that the kinetics of partial melting in a β-spodumene glass–ceramic is apparently limited by the diffusion rate of silica in the crystal and the lattice diffusivity of silica is $8\times10^{-10}\times\exp(-251\,\text{kJ/mol}\cdot(1/RT))\,\text{m}^2/\text{s}$ with a possible error of 60 kJ/mol in the activation energy. The nucleation and crystallization of a $61SiO_2{\cdot}6Al_2O_3{\cdot}10MgO{\cdot}6ZnO{\cdot}12Li_2O{\cdot}5TiO_2$ (in mol%) glass have been investigated by Barbieri et al. [18] using differential thermal analysis (DTA) and differential scanning calorimetry (DSC) methods. Several methods have been proposed to obtain kinetics data from DTA, DSC curves [18–23] and XRD results [13,24,25].

In the present study, the crystallization behavior of the $(1-x)Li_2O{\cdot}xNa_2O{\cdot}Al_2O_3{\cdot}4SiO_2$ glasses has been investigated by X-ray diffraction (XRD), scanning electron microscopy (SEM), transmission electron microscopy (TEM) and electron diffraction (ED). The crystallization kinetics and mechanism of the $(1-x)Li_2O{\cdot}xNa_2O{\cdot}Al_2O_3{\cdot}4SiO_2$ glasses have been discussed in detail.

* Corresponding author. Tel.: +886 37 381707; fax: +886 37 324047.
E-mail address: chsi@nuu.edu.tw (C.-S. Hsi).

0925-8388/$ – see front matter
doi:10.1016/j.jallcom.2010.04.048

Table 1
Stoichiometry of $(1-x)Li_2O{\cdot}xNa_2O{\cdot}Al_2O_3{\cdot}4SiO_2$ glasses.

Sample	Chemical composition (mol)			
	Li_2O	Na_2O	Al_2O_3	SiO_2
C_1 ($x=0$)	1	0	1	4
C_2 ($x=0.2$)	0.8	0.2	1	4
C_3 ($x=0.4$)	0.6	0.4	1	4
C_4 ($x=0.5$)	0.5	0.5	1	4
C_5 ($x=0.6$)	0.4	0.6	1	4
C_6 ($x=0.8$)	0.2	0.8	1	4
C_7 ($x=1$)	0	1	1	4

2. Experimental procedures

2.1. Glass preparation

Reagent-grade powders of Li_2CO_3 (Nippon Shiyaku Kogyo KK, Ltd., Osaka, Japan), Na_2CO_3 (Nippon Shiyaku Kogyo KK, Ltd., Osaka, Japan), Al_2O_3 (Nippon Shiyaku Kogyo KK, Ltd., Osaka, Japan) and SiO_2 (Nacalai Tesque, Ltd., Kyoto, Japan) were used as raw materials for preparing the $(1-x)Li_2O{\cdot}xNa_2O{\cdot}Al_2O_3{\cdot}4SiO_2$ glasses. The compositions of these glasses are listed in Table 1. Na_2O was added in 0.2 mol stepwise substitution for Li_2O in the $(1-x)Li_2O{\cdot}xNa_2O{\cdot}Al_2O_3{\cdot}4SiO_2$ glasses except C_4. All samples were obtained in a 200 g batch by melting in a platinum crucible at 1773 K in an electric furnace for 2 h. After homogenizing, the melt was quenched in water and dried. The crushed powders were remelted at 1773 K for another 2 h, then cast onto a hot stainless steel plate at 673 K, and transferred to an annealing furnace at 673 K for 2–4 h. Finally, a clear, transparent, colorless glass was obtained.

2.2. Sample characterization

The crystalline phases were identified by XRD with Cu K_α radiation and a Ni filter operated at 30 kV, 20 mA and a scanning rate of 0.25° min^{-1} (Model Rad II A, Rigaku, Tokyo, Japan). The XRD amount of each constituent quantitative was determined by the powder method [26–28]. The amount of β-spodumene present in the glass was determined by comparing the intensity of its major peak (2θ from 24.5° to 26.1°) of the β-spodumene with the standard. The standard specimen was made by the sol–gel method [29] and the LAS gels were calcined at 1623 K for 24 h. A scanning electron microscope (SEM, Hitachi S3000N, Tokyo, Japan) was used to observe the surface of the polished sample, etched with a solution of 5 parts HF, 2 parts HCl and 93 parts H_2O and coated with a thin gold film.

The microstructure and morphology of the crystallized sample were examined with a transmission electron microscope (Hitachi model HF-2000, Hitachi Ltd., Tokyo, Japan) operated at 200 kV. Electron diffraction (ED) examination was also made on a carefully thinned foil of the crystallized sample. A disk with a diameter of 3 mm was sliced from the bulk with an ultrasonic cutter and mechanically thinned to a thickness of 80 μm or less, employing a diamond paste. The final thinning was done by ion-milling to electron transparency.

2.3. Method of isothermal crystallization and growth

For the crystallization of a glass, the nucleation and crystal growth may occur simultaneously, for which the Johnson–Mehl–Avrami (JMA) equation [29,30] has been developed to describe the kinetics of the process as follows.

$$\ln\left(\frac{1}{1-x}\right) = (kt)^n \tag{1}$$

where x is the crystallization fraction for heating time t, n is the growth morphology parameter and k is the rate constant related to an Arrhenius' equation:

$$k = A\ \exp\left(-\frac{E_a}{RT}\right) \tag{2}$$

where E_a is the activation energy, R is the gas constant, T is the absolute temperature and A is a constant.

Eq. (3) is obtained by taking the logarithms of both sides of Eq. (1).

$$\ln\left[\ln\left(\frac{1}{1-x}\right)\right] = n\ \ln k + n\ \ln t \tag{3}$$

Eq. (4) is obtained by taking the logarithms of both sides of Eq. (2)

$$\ln\ k = \ln A - \frac{E_a}{RT} \tag{4}$$

In the present study the crystallization temperatures from 1153 to 1363 K.

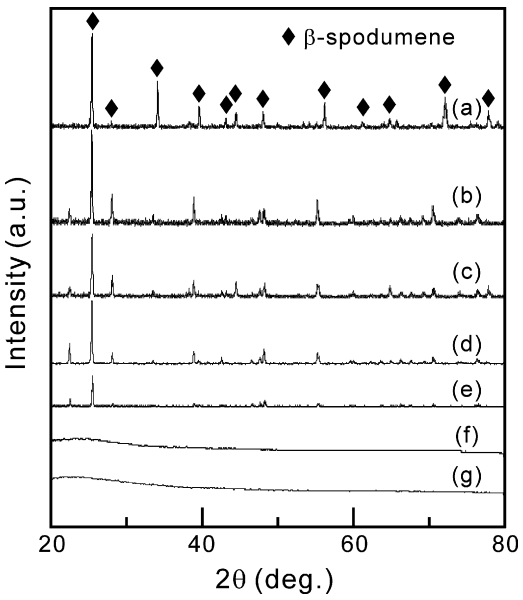

Fig. 1. XRD patterns of $(1-x)Li_2O{\cdot}xNa_2O{\cdot}Al_2O_3{\cdot}4SiO_2$ ($0 \le x \le 1$) glasses crystallized at 1263 K for 2 h: (a) C_1 ($x=0$), (b) C_2 ($x=0.2$), (c) C_3 ($x=0.4$), (d) C_4 ($x=0.5$), (e) C_5 ($x=0.6$), (f) C_6 ($x=0.8$) and (g) C_7 ($x=1.0$).

3. Results and discussion

3.1. The phase of $(1-x)Li_2O{\cdot}xNa_2O{\cdot}Al_2O_3{\cdot}4SiO_2$ glasses after crystallization

Fig. 1 illustrates the XRD patterns of the glass samples C_1 ($x=0$) to C_5 ($x=0.6$) crystallized at 1263 K for 2 h. The d-spacings of the principal crystalline phase were identical to that of β-spodumene ($Li_2O{\cdot}Al_2O_3{\cdot}4SiO_2$). Fig. 1(f) and (g) demonstrates that the glass samples of the C_6 ($0.2Li_2O{\cdot}0.8Na_2O{\cdot}Al_2O_3{\cdot}4SiO_2$) and C_7 ($Na_2O{\cdot}Al_2O_3{\cdot}4SiO_2$) still remain as glassy after crystallization at 1263 K for 2 h. Moreover, the intensity of the XRD patterns of the β-spodumene decreases with increasing Na_2O content. This results were attributed to the glass samples C_6 and C_7 reduction of Li_2O concentration, as a constituent of β-spodumene crystals, by gradual substitution of Li_2O by Na_2O.

In the $(1-x)Li_2O{\cdot}xNa_2O{\cdot}Al_2O_3{\cdot}4SiO_2$ glasses system, the DTA results show that the crystallization temperatures (T_c) slightly increase from 1171.2 to 1172.6 K when the Na_2O content increased from 0 to 0.2 mol (i.e. C_1 and C_2 glasses). Moreover, the T_c abrupt increases from 1186.7 to 1212.4 K when the Na_2O content increased from 0.4 to 0.6 mol (i.e. C_3, C_4 and C_5 glasses) [16]. Hence, the crystallization process temperatures can be divided into two groups: (i) from 1153 to 1273 K for C_1 and C_2 glasses and (ii) from 1273 to 1363 K for C_3, C_4 and C_5 glasses. The relations between the relative volume of the β-spodumene and the crystallization temperature for C_1 to C_5 are shown in Fig. 2. The formation of the β-spodumene increases with increasing crystallization temperature and time for each glass, however, it decreases with increasing Na_2O content.

3.2. Kinetics of β-spodumene formation from $(1-x)Li_2O{\cdot}xNa_2O{\cdot}Al_2O_3{\cdot}4SiO_2$ glasses

When $\ln[\ln(1/(1-x))]$ was plotted against $\ln t$, as shown in Fig. 3, the straight lines n are the growth morphology parameters of the β-spodumene phase as listed in Table 2. It was found that the n value decreases from 1.86 to 1.20 for the C_1 glass when the crystallization temperature increases from 1153 to 1243 K. Fig. 3 also indicates that the variation of the crystallization morphology parameter with crystallization temperature of the glass samples C_2 to C_5 was as

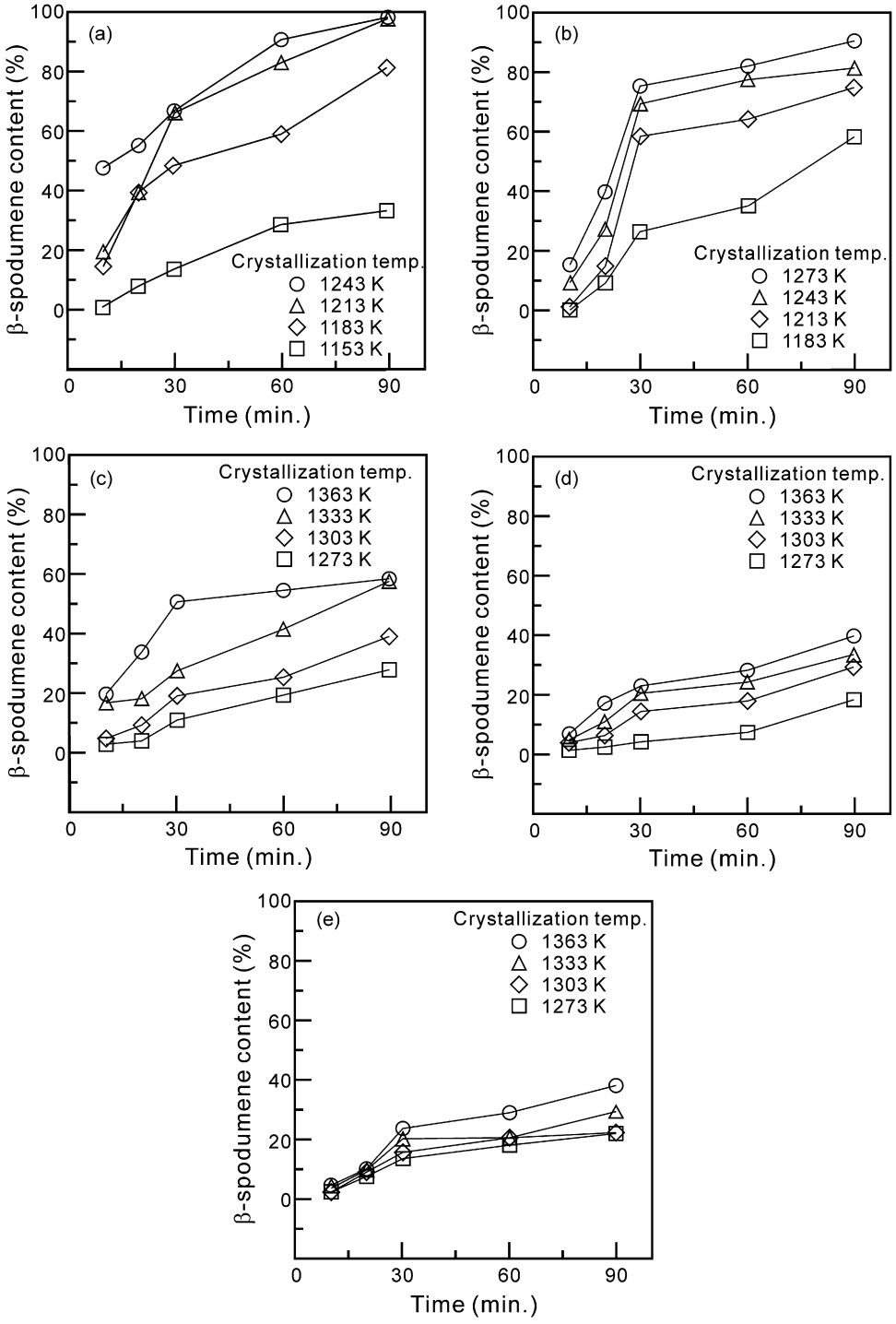

Fig. 2. Relation between β-spodumene content, crystallization temperatures and times of $(1-x)Li_2O{\cdot}xNa_2O{\cdot}Al_2O_3{\cdot}4SiO_2$ $(0 \le x \le 1)$ glasses. (a) C_1 ($x=0$), (b) C_2 ($x=0.2$), (c) C_3 ($x=0.4$), (d) C_4 ($x=0.5$), and (e) C_5 ($x=0.6$).

Table 2
The growth morphology parameter n of $(1-x)Li_2O{\cdot}xNa_2O{\cdot}Al_2O_3{\cdot}4SiO_2$ glasses crystallization at various temperatures.

C_1 ($x=0$)		C_2 ($x=0.2$)		C_3 ($x=0.4$)		C_4 ($x=0.5$)		C_5 ($x=0.6$)	
Temperature (K)	n_i	Temperature (K)	n_i	Temperature (K)	n_i	Temperature (K)	n_i	Temperature (K)	n_i
1153	1.86	1183	1.81	1273	1.82	1273	2.05	1273	1.67
1183	1.70	1213	1.56	1303	1.74	1303	1.73	1303	1.62
1213	1.42	1243	1.50	1333	1.60	1333	1.44	1333	1.47
1243	1.20	1273	1.41	1363	1.59	1363	1.42	1363	1.21

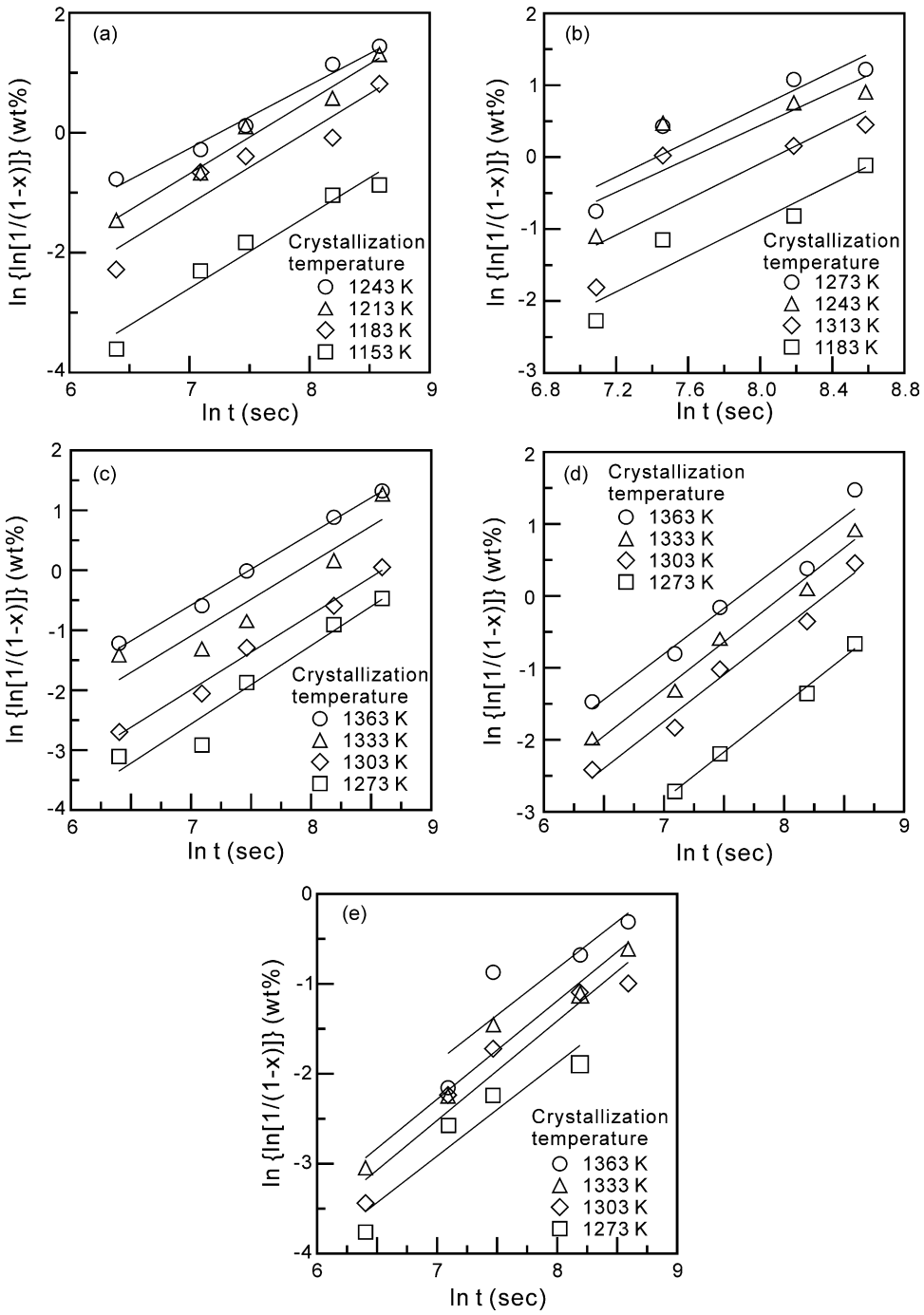

Fig. 3. Plot of $\ln[\ln(1/(1-x))]$ as a function of $\ln k$ for $(1-x)Li_2O{\cdot}xNa_2O{\cdot}Al_2O_3{\cdot}4SiO_2$ ($0 \le x \le 0.6$) glasses. (a) C_1 ($x=0$), (b) C_2 ($x=0.2$), (c) C_3 ($x=0.4$), (d) C_4 ($x=0.5$), and (e) C_5 ($x=0.6$).

same as the C_1 glass. Moreover, Fig. 3 also provides the kinetic constant data k from the intercept of the straight line with the axis of $\ln[\ln(1/(1-x))]$.

The left side of Eq. (4), $\ln k$, is plotted against the reciprocal crystallization temperature, $1/T$, in Fig. 4, to obtain the apparent activation energy from the slope. The apparent activation energy depends on the Na_2O content as shown in Fig. 5. It was found that the activation energy for the β-spodumene crystallization decreases from 359.2 to 317.8 kJ/mol when the Na_2O content increases from 0 to 0.4 mol and then increases from 317.8 to 376.9 kJ/mol when the Na_2O content increases from 0.4 to 0.6 mol.

According to the results of Figs. 2 and 5, although the minimum activation energy of $(1-x)Li_2O{\cdot}xNa_2O{\cdot}Al_2O_3{\cdot}4SiO_2$ glasses crystallization as 317.8 kJ/mol when the Na_2O content is 0.4 mol (i.e. C_3 glass), but the β-spodument content was not maximum for C_3 glass. This result may be caused by the T_c which increases with the Na_2O content increased from 0 to 0.6 mol (i.e. for C_1 to C_5 glasses), but the T_c of C_6 and C_7 does not appear when the Na_2O contents are 0.8 and 1.0 mol due to the abrupt change of the dilatometric softening temperatures [16]. In the present study, at the crystallization process, the viscosity of residual glass increases with the Na_2O content increasing, which inhibited the β-sprodumene formation, and results in that the β-sprodumene

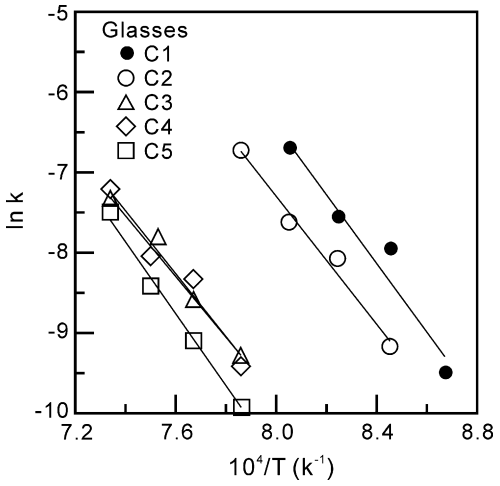

Fig. 4. ln k vs. $1/T$ for $(1-x)Li_2O{\cdot}xNa_2O{\cdot}Al_2O_3{\cdot}4SiO_2$ $(0 \le x \le 0.6)$ glasses.

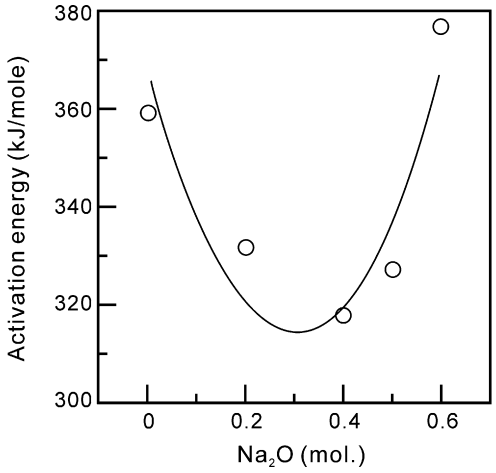

Fig. 5. Activation energy for β-spodumene formation from various $(1-x)Li_2O{\cdot}xNa_2O{\cdot}Al_2O_3{\cdot}4SiO_2$ glasses $(0 \le x \le 0.6)$.

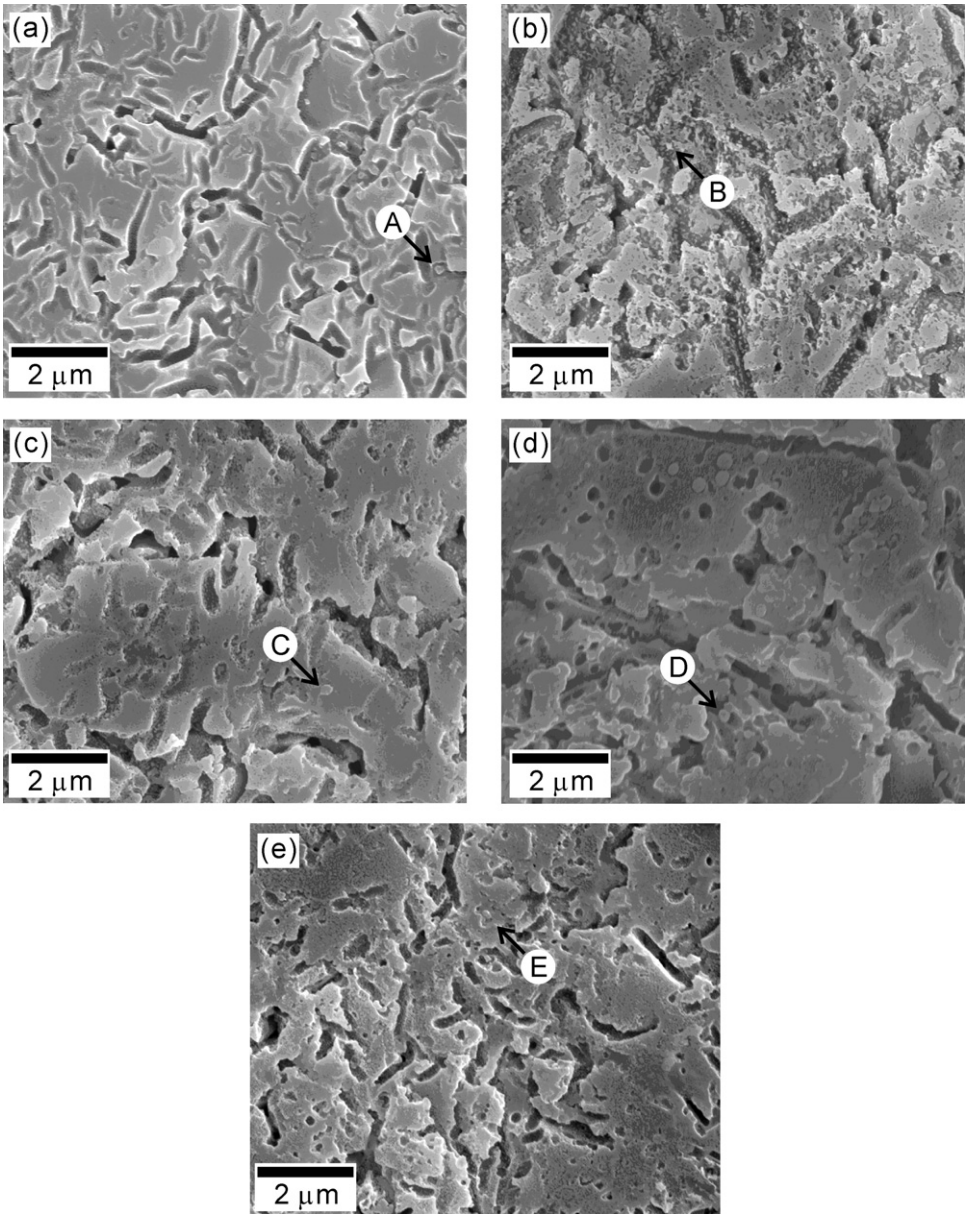

Fig. 6. Surface morphology of $(1-x)Li_2O{\cdot}xNa_2O{\cdot}Al_2O_3{\cdot}4SiO_2$ glasses crystallized at 1263 K for 2 h: (a) C_1 ($x=0$), (b) C_2 ($x=0.2$), (c) C_3 ($x=0.4$), (d) C_4 ($x=0.5$), and (e) C_5 ($x=0.6$).

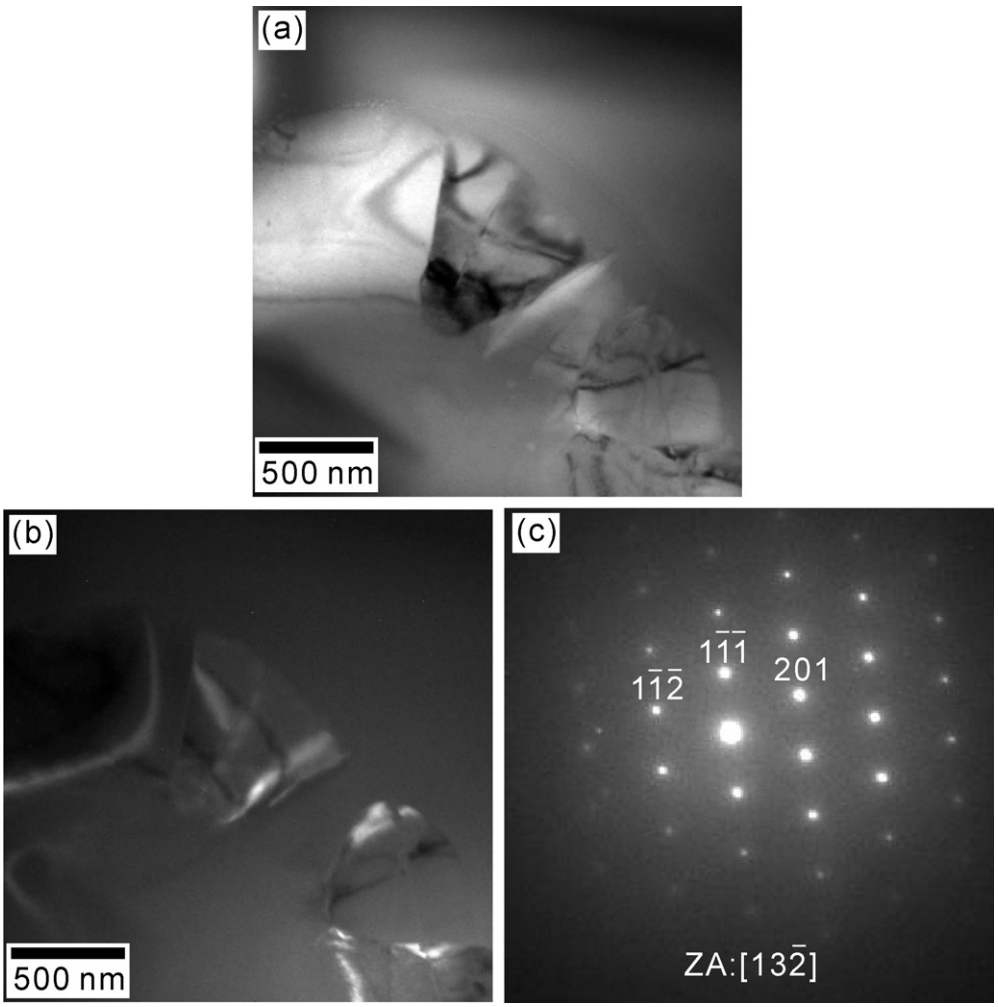

Fig. 7. TEM micrographs and ED pattern of C_1 ($Li_2O{\cdot}Al_2O_3{\cdot}4SiO_2$) glasses crystallized at 1123 K for 2 h: (a) BF image, (b) DF image, and (c) ED pattern of β-spodumene.

content decreases with the Na_2O content increasing. Wang et al. [16] and Tomozawa [31] have pointed out that the alkali ion mobility in oxide glasses decreases drastically when x exceeds 0.4 mol causing an increase in activation energy as shown in Fig. 5.

3.3. *Microstructure of $(1-x)Li_2O{\cdot}xNa_2O{\cdot}Al_2O_3{\cdot}4SiO_2$ glasses after crystallization*

The SEM micrographs of various glass samples (C_1 to C_5) crystallized at 1263 K for 2 h are illustrated in Fig. 6. The crystals of β-spodumene were observed in these samples after crystallization as shown by A–E in Fig. 6(a)–(c), respectively. The chemical compositions of A–E in Fig. 6(a)–(c), respectively, are listed in Table 3, indicating that the crystals contain Na_2O except for A (C_1 sample).

Table 3
Chemical compositions at various locations in Fig. 6 determined SEM–EDS.

Element	Chemical composition (at.%)				
	A (C_1)	B (C_2)	C (C_3)	D (C_4)	E (C_5)
Na	–	0.86	0.93	1.64	2.53
Al	12.63	14.49	10.83	11.23	10.64
Si	28.99	34.47	24.44	24.58	24.43
O	58.36	50.17	63.80	62.56	62.41

In conjunction with the XRD analysis, the bright-field (BF) and dark-field (DF) images of TEM together with the corresponding electron diffractions (ED) have been carried out. Fig. 7 shows the individual single crystal with a plate-like morphology after growth without branching for the C_1 glass crystallized at 1123 K for 2 h. The ED pattern (Fig. 7(c)) also provides the evidence for the formation of the β-spodumene crystal.

Fig. 8 illustrates the C_2 glasses crystallized at 1123 K for 6 h, it also indicates the plate-like morphology of the β-spodumene. Figs. 8 (a) and (b) shows the wide and long of crystals about 130.0 and 200.0 nm, respectively. Fig. 8(c) shows the ED pattern of the β-spodumene. The product of the C_2 sample crystallized at 1123 K for 6 h was identified to be the β-spodumene and no other phase was found. Fig. 8(d) demonstrates the EDS result of the individual single crystal marked A in Fig. 8(a), showing the β-spodumene crystal is formed in the C_2 glass sample containing Na_2O.

From the results of Fig. 3 and Table 2, it was found that the crystallization parameter n decreases with increasing Na_2O content. This phenomenon suggests that Na_2O content increases the matrix viscosity and reduces the crystal growth rate, hence the morphology of the β-spodumene crystal tends to be elongated and causes decreasing parameter n.

The result of Figs. 7 and 8 may be partly due to the impinging small crystals and the enhanced isotropy in growth is aided by the presence of the phase-separated β-spodumene droplets which are enveloped by the growing crystals.

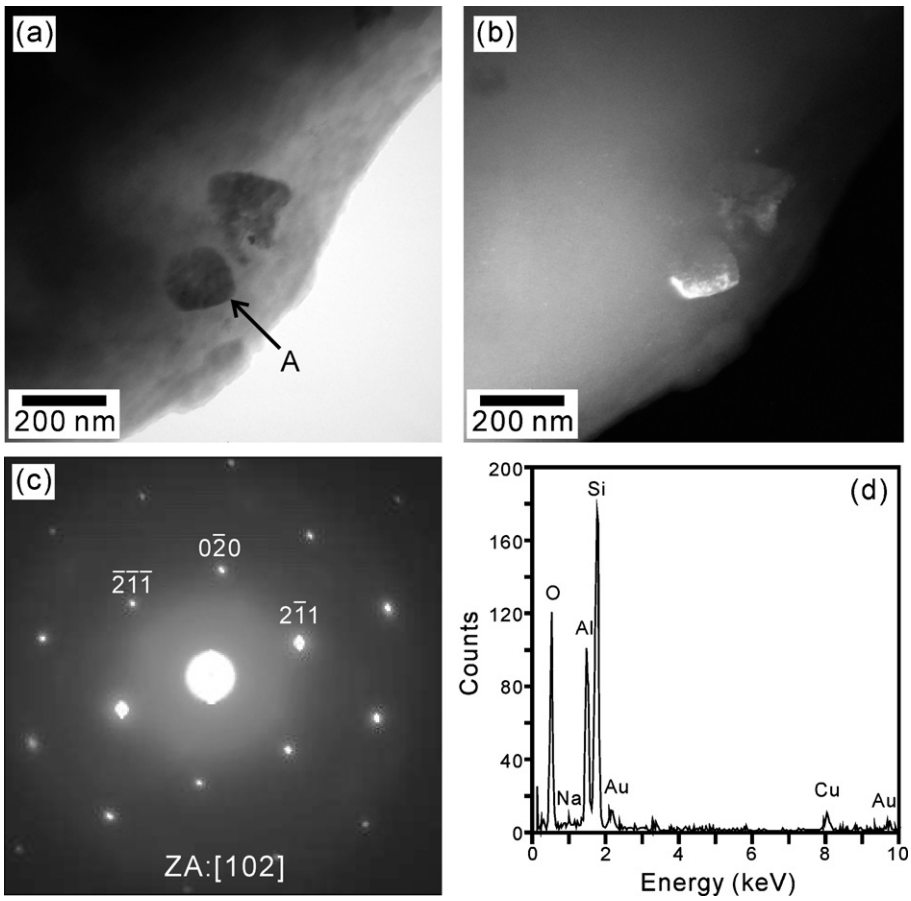

Fig. 8. TEM micrographs and ED pattern of C_2 glass crystallized at 1123 K for 6 h: (a) BF image, (b) DF image, (c) ED pattern of β-spodumene, and (d) EDS result of location marked by A in (a).

4. Conclusions

The crystallization behavior of $(1-x)Li_2O{\cdot}xNa_2O{\cdot}Al_2O_3{\cdot}4SiO_2$ glasses have been investigated. The results were summarized as follows:

(1) The crystalline phase was identified as β-spodumene for $(1-x)Li_2O{\cdot}xNa_2O{\cdot}Al_2O_3{\cdot}4SiO_2$ $(0 \le x \le 0.6)$ glasses after crystallization at 1263 K for 2 h, but $(1-x)Li_2O{\cdot}xNa_2O{\cdot}Al_2O_3{\cdot}4SiO_2$ $(0.8 \le x \le 1)$ glasses still maintain the amorphous state.
(2) A modified version of the JMA equation with the crystallization morphology parameter of about 2 shows a plate-like crystallization mode of β-spodumene from the $(1-x)Li_2O{\cdot}xNa_2O{\cdot}Al_2O_3{\cdot}4SiO_2$ $(0 \le x \le 0.6)$ glasses.
(3) The activation energy of crystallization decreases from 359.2 to 317.8 kJ/mol when the Na_2O content (x) increases from 0 to 0.4, and then increases from 317.8 to 376.9 kJ/mol when the x value increases from 0.4 to 0.6.
(4) The β-spodumene crystal formed from $(1-x)Li_2O{\cdot}xNa_2O{\cdot}Al_2O_3{\cdot}4SiO_2$ $(0 \le x \le 0.6)$ glasses.

Acknowledgments

This work was supported by the National Science Council, Taiwan, under Contract No. NSC 92-2216-E-230-002. The authors sincerely thank Prof. M.P. Hung for manuscript discussion, Mr. J.M. Chen and Mr. S.Y. Yao for assistance in XRD and SEM.

References

[1] H. Scheilder, E. Rodek, Am. Ceram. Soc. Bull. 68 (1989) 1926–1930.
[2] M. Guides, A.C. Ferro, J.M.F. Ferreira, J. Eur. Ceram. Soc. 21 (2001) 1187–1194.
[3] Z. Strnad, Glass Science and Technology, Glass Ceramic Materials, 8, Elsevier, Amsterdam, Netherlands, 1986, p. 85.
[4] S. Knickerbocker, M.R. Tuzzolo, S. Lawhorne, J. Am. Ceram. Soc. 72 (1989) 1879–1973.
[5] J.Y. Hsu, R.F. Speyer, J. Am. Ceram. Soc. 72 (1989) 2334–2341.
[6] W. Ostertag, G.R. Fischer, J.P. Williams, J. Am. Ceram. Soc. 51 (1968) 651–654.
[7] P.E. Doherty, D.W. Lee, R.S. Davis, J. Am. Ceram. Soc. 50 (1976) 77–81.
[8] G. Partridge, Glass Technol. 23 (1982) 133–138.
[9] J.Y. Hsu, R.F. Speyer, J. Am. Ceram. Soc. 73 (1990) 3585–3593.
[10] J.Y. Hsu, R.F. Speyer, J. Am. Ceram. Soc. 74 (1991) 395–399.
[11] M.L. Wang, R. Stevents, P. Kuott, Glass Technol. 23 (1982) 238–243.
[12] A.V.A. El-Shennawi, A.A. Omar, A.R. El-Ghannam, Ceram. Int. 17 (1991) 25–29.
[13] M.C. Wang, M.H. Hon, J. Ceram. Soc. Jpn. 100 (1992) 1285–1291.
[14] M.C. Wang, M.H. Hon, Ceram. Int. 19 (1993) 223–230.
[15] M.C. Wang, M.H. Hon, J. Mater. Res. 8 (1993) 890–898.
[16] M.C. Wang, C.W. Cheng, P.Y. Shih, C.S. Hsi, J. Non-Cryst. Solids 353 (2007) 2295–2300.
[17] K.H. Dalal, R. Raj, J. Am. Ceram. Soc. 64 (1981) 194–200.
[18] L. Barbieri, C. Leononelli, T. Manfredini, C. Siligardi, A.B. Corradi, P. Mustarelli, C. Tomasi, J. Am. Ceram. Soc. 80 (1997) 3077–3083.
[19] M.D. Baro, N. Clawaguerea, S. Bordas, M.T. Cavagera-Mora, J. Casas-Vazquez, J. Therm. Anal. 11 (1977) 271–276.
[20] F. Branda, A. Buri, A. Marotta, S. Saiello, Thermochim. Acta 80 (1984) 269–274.
[21] C.S. Ray, W. Huang, D.E. Day, J. Am. Ceram. Soc. 74 (1991) 60–66.
[22] S. Yannacopoulos, S.O. Kasap, J. Mater. Res. 5 (1990) 789–794.
[23] C.S. His, M.C. Wang, J. Mater. Res. 13 (1998) 2655–2661.
[24] S.W. Freiman, L.L. Hench, J. Am. Ceram. Soc. 51 (1968) 382–387.
[25] W.A. Zdaniewski, J. Am. Ceram. Soc. 61 (1978) 199–204.
[26] Y.F. Chen, M.C. Wang, M.H. Hon, J. Mater. Res. 18 (2003) 1355–1362.
[27] Y.F. Chen, M.C. Wang, M.H. Hon, Scripta Mater. 51 (2004) 231–235.
[28] S.B. Wen, N.C. Wu, S. Yang, M.C. Wang, J. Mater. Res. 14 (1999) 3559–3566.
[29] M.E. Fine, Introduction to Phase Transformations in Condensed Systems, The Macmillan Company, New York, 1964, p. 75.
[30] R.V. Muraleedharan, J. Therm. Anal. 37 (1991) 2729–2730.
[31] M. Tomozawa, J. Non-Cryst. Solids 152 (1993) 59–69.